

Discrete adjoint approximations with shocks

Michael B. Giles
giles@comlab.ox.ac.uk
Oxford University Computing Laboratory, Oxford OX1 3QD

This paper is concerned with the formulation and discretisation of adjoint equations when there are shocks in the underlying solution to the original nonlinear hyperbolic p.d.e. For the model problem of a scalar unsteady one-dimensional p.d.e. with a convex flux function, it is shown that the analytic formulation of the adjoint equations requires the imposition of an interior boundary condition along any shock. A 'discrete adjoint' discretisation is defined by requiring the adjoint equations to give the same value for the linearised functional as a linearisation of the original nonlinear discretisation. It is demonstrated that convergence requires increasing numerical smoothing of any shocks. Without this, any consistent discretisation of the adjoint equations without the inclusion of the shock boundary condition may yield incorrect values for the adjoint solution.

Oxford University Computing Laboratory
Numerical Analysis Group
Wolfson Building
Parks Road
Oxford, England OX1 3QD

July, 2002

1 Introduction

In recent years there has been considerable research into the use of adjoint flow equations for design optimisation (e.g. [Jam95, AV99, GP00]) and error analysis (e.g. [JRB95, MS98, PG00, BR01]). In almost every case, the adjoint equations have been formulated under the assumption that the original nonlinear flow solution is smooth. Since most applications have been for incompressible or subsonic flow, this has been valid, however there is now increasing use of such techniques in transonic design applications for which there are shocks. It is therefore of interest to investigate the formulation and discretisation of adjoint equations when in the presence of shocks.

The reason that shocks present a problem is that the adjoint equations are defined to be adjoint to the equations obtained by linearising the original nonlinear flow equations. Therefore, this raises the whole issue of linearised perturbations to the shock. The analysis will show how the analytic treatment must correctly linearise the shock jump equations which arise from conservation properties at the shock. However, for the numerical approximation it is not clear whether the linearised shock capturing will yield the correct results.

The validity of linearised shock capturing for harmonically oscillating shocks in flutter analysis was investigated by Lindquist and Giles [LG94] who showed that the shock capturing produces the correct prediction of integral quantities such as unsteady lift and moment provided the shock is smeared over a number of grid points. One interpretation of this is that it ensures the “viscous” shock profile remains invariant, to a very good approximation, as the shock oscillates, and therefore the integral effect of the linearised shock motion is correct. As a result, linearised shock capturing is now the standard method of turbomachinery aeroelastic analysis [HCL94, SW98], benefitting from the computational advantages of the linearised approach, without the many drawbacks of shock fitting.

There has been very little prior research into adjoint equations for flows with shocks. Giles and Pierce [GP01] have shown that the analytic derivation of the adjoint equations for the steady quasi-one-dimensional Euler equations requires the specification of an internal adjoint boundary condition at the shock. However, the numerical evidence [GP98] is that the correct adjoint solution is obtained using either the “fully discrete” approach (in which one linearises the discrete equations and uses the transpose) or the “continuous” approach (in which one discretises the analytic adjoint equations). In the case of the fully discrete approach, this is due to the second order accuracy of conservative quasi-one-dimensional shock capturing [Gil96], whereas with the continuous approach it is thought to be because the use of numerical smoothing automatically selects the correct numerical solution which is smooth at the shock [GP98]. It is not clear though that either approach will produce the correct results in two dimensions, for which there is a similar adjoint boundary condition along a shock.

In this paper, which is an expanded version of [Gil02], we consider unsteady one-dimensional hyperbolic equations with a convex scalar flux, and in particular obtain numerical results for Burgers equation. Tadmor [Tad91] developed a Lip’ topology for the formulation of adjoint equations for this problem, with application to linear post-

processing functionals. Building on this and the work of Bouchut and James [BJ98], Ulbrich has very recently introduced the concept of shift-differentiability [Ul02a, Ul02b] to handle nonlinear functionals of the type considered in this paper. However, in this paper we will provide an alternative derivation of the analytic adjoint solution against which the numerical solutions will be compared.

We start by deriving the analytic adjoint equations for the case when the underlying solution is smooth, and then present the extension to handle the presence of a shock. It is shown that the latter requires the imposition of an interior boundary condition along any shock. The numerical discretisation is formulated by following the 'fully discrete' approach, requiring the adjoint equations to give exactly the same value for the linearised functional as a linearisation of the original nonlinear discretisation. It is demonstrated that using consistent, conservative numerical Riemann flux function yields incorrect values for the adjoint solution when there is a shock. However, a simpler Lax-Friedrichs flux formulation with numerical smoothing yields convergent values if the shock is spread over an increasing number of points.

2 Analytic formulation in the absence of shocks

Let $u(x, t)$ be the solution of the scalar equation

$$\frac{\partial u}{\partial t} + \frac{\partial f(u)}{\partial x} = 0, \quad 0 < x < 1, \quad 0 < t < T$$

subject to initial conditions $u(x, 0) = u_0(x)$. Numerical results will be presented later for the Burgers equation for which $f(u) \equiv \frac{1}{2}u^2$, but here we consider a general convex function $f(u)$. If the solution $u(x, t)$ is differentiable, then

$$\frac{\partial u}{\partial t} + \frac{df}{du} \frac{\partial u}{\partial x} = 0.$$

It follows from this that $u(x, t)$ is constant along straight characteristics defined by

$$\frac{dx}{dt} = \frac{df}{du}.$$

We will assume that $df/du > 0$ at $x=0$ and $df/du < 0$ at $x=1$, and therefore the value of $u(x, t)$ is specified on the two side boundaries.

We now consider a linear perturbation \tilde{u} . The linearised p.d.e. with the addition of a perturbation source term s is

$$\frac{\partial \tilde{u}}{\partial t} + \frac{\partial}{\partial x} \left(\frac{df}{du} \tilde{u} \right) = s. \quad (2.1)$$

If the boundary conditions are not perturbed, then $\tilde{u}=0$ on $t=0$, $x=0$ and $x=1$.

If one is interested in an output functional

$$J(u) = \int_0^1 G(u(x, T)) \, dx,$$

with $G(u)$ being a function with a continuous derivative, then the linearised functional perturbation is

$$\tilde{J} = \int_0^1 g(x) \tilde{u}(x, T) dx.$$

where $g(x) = dG/du(x, T)$. Using integration by parts, this can be re-expressed using any differentiable function $v(x, t)$ as

$$\begin{aligned} \tilde{J} &= \int_0^1 g(x) \tilde{u}(x, T) dx - \iint_{\Omega} v \left(\frac{\partial \tilde{u}}{\partial t} + \frac{\partial}{\partial x} \left(\frac{df}{du} \tilde{u} \right) - s \right) dx dt \\ &= \int_0^1 (g(x) - v(x, T)) \tilde{u}(x, T) dx + \iint_{\Omega} \left(\frac{\partial v}{\partial t} + \frac{df}{du} \frac{\partial v}{\partial x} \right) \tilde{u} dx dt + \iint_{\Omega} v s dx dt \end{aligned}$$

If v is defined to satisfy the adjoint equation

$$\frac{\partial v}{\partial t} + \frac{df}{du} \frac{\partial v}{\partial x} = 0, \quad (2.2)$$

subject to the final condition $v(x, T) = g(x)$, then this reduces to

$$\tilde{J} = \iint_{\Omega} v s dx dt, \quad (2.3)$$

which can be evaluated without knowing \tilde{u} . This is the basis of the use of adjoint solutions in both design optimisation and error analysis for specific output functionals.

In the specific case when $s(x, t)$ is a Dirac delta function

$$s(x, t) = \delta(x - x_0) \delta(t - t_0)$$

then we obtain

$$\tilde{J} = v(x_0, t_0).$$

Thus, one interpretation of the adjoint solution $v(x_0, t_0)$ is that it is the linearised functional obtained when the linearised equation are subject to a unit strength point source at (x_0, t_0) . For such a source term, the linear perturbation \tilde{u} is zero except on the characteristic passing through (x_0, t_0) . To determine the value along this characteristic, we integrate equation (2.1) over Ω and use the initial and boundary conditions to obtain

$$\int_0^1 \tilde{u}(x, T) dx = 1,$$

and hence

$$\tilde{u}(x, T) = \delta(x - x_1),$$

where x_1 is the intersection point of the characteristic with the final boundary $t = T$. The corresponding perturbed functional is

$$v(x_0, t_0) \equiv \tilde{J} = g(x_1),$$

so this provides confirmation by this alternative derivation that the value of the adjoint solution is propagated unchanged along the backward travelling characteristic.

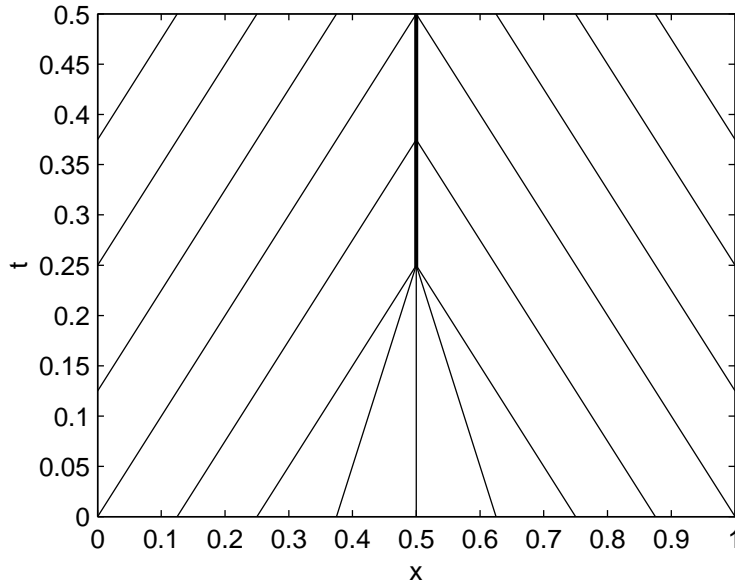


Figure 1: Characteristics with a shock forming along $x=0.5$.

3 Analytic formulation with a shock

What happens when there is a shock along a curve $\Gamma = (t, x_s(t))$ from $t=0$ to $t=T$, as illustrated in Figure 1?

Firstly, the velocity of the shock is given by

$$\frac{dx_s}{dt} [u] = [f(u)],$$

where $[\cdot]$ denotes the jump in the quantity across the shock [LeV92].

The linearised equation remains the same in the region $\Omega \setminus \Gamma$ omitting the shock itself. In addition to this, one must linearise the shock velocity equation with respect to changes in $x_s(t)$ as well as $u(x, t)$, giving

$$\frac{d\tilde{x}_s}{dt} [u] + \frac{dx_s}{dt} [\tilde{u}] + \frac{dx_s}{dt} \tilde{x}_s \left[\frac{\partial u}{\partial x} \right] = \left[\frac{df}{du} \tilde{u} \right] + \tilde{x}_s \left[\frac{df}{du} \frac{\partial u}{\partial x} \right].$$

The linearised functional also needs to be modified to take into account the effect of the displaced shock. Writing the nonlinear functional as

$$J = \int_0^{x_s(T)} G(u(x, T)) dx + \int_{x_s(T)}^1 G(u(x, T)) dx,$$

it follows that

$$\tilde{J} = \int_0^{x_s(T)} g(x) \tilde{u}(x, T) dx + \int_{x_s(T)}^1 g(x) \tilde{u}(x, T) dx - (\tilde{x}_s [G])|_{t=T}.$$

Now, introducing a new variable v_s for the linearised shock equation, and again integrating by parts over $\Omega \setminus \Gamma$, gives

$$\begin{aligned}
\tilde{J} &= \int_0^{x_s(T)} g(x) \tilde{u}(x, T) dx + \int_{x_s(T)}^1 g(x) \tilde{u}(x, T) dx - (\tilde{x}_s [G])|_{t=T} \\
&\quad - \iint_{\Omega \setminus \Gamma} v \left(\frac{\partial \tilde{u}}{\partial t} + \frac{\partial}{\partial x} \left(\frac{df}{du} \tilde{u} \right) - s \right) dx dt \\
&\quad + \int_{\Gamma} v_s \left(\frac{d\tilde{x}_s}{dt} [u] + \frac{dx_s}{dt} [\tilde{u}] + \frac{dx_s}{dt} \tilde{x}_s \left[\frac{\partial u}{\partial x} \right] - \left[\frac{df}{du} \tilde{u} \right] - \tilde{x}_s \left[\frac{df}{du} \frac{\partial u}{\partial x} \right] \right) dt \\
&= \int_0^{x_s(T)} (g(x) - v(x, T)) \tilde{u}(x, T) dx + \int_{x_s(T)}^1 (g(x) - v(x, T)) \tilde{u}(x, T) dx \\
&\quad - (\tilde{x}_s [G])|_{t=T} + \iint_{\Omega \setminus \Gamma} \left(\frac{\partial v}{\partial t} + \frac{df}{du} \frac{\partial v}{\partial x} \right) \tilde{u} + v s dx dt - \int_{\Gamma} [v\tilde{u}] dx - \left[v \frac{df}{du} \tilde{u} \right] dt \\
&\quad + \int_0^T v_s \left(\frac{d\tilde{x}_s}{dt} [u] + \frac{dx_s}{dt} [\tilde{u}] + \frac{dx_s}{dt} \tilde{x}_s \left[\frac{\partial u}{\partial x} \right] - \left[\frac{df}{du} \tilde{u} \right] - \tilde{x}_s \left[\frac{df}{du} \frac{\partial u}{\partial x} \right] \right) dt
\end{aligned}$$

Noting that $dx = dx_s/dt dt$ along Γ , all of the terms involving \tilde{u} are either zero or cancel out if $v(x, t)$ is again defined to satisfy the adjoint equation (2.2) in $\Omega \setminus \Gamma$, together with the same final conditions on $t=T$, plus the additional constraint that on Γ , $v = v_s$ on either side of the shock.

Applying integration by parts to the terms involving \tilde{x}_s yields

$$\begin{aligned}
&- (\tilde{x}_s [G])|_{t=T} + \int_{\Gamma} v_s \left(\frac{d\tilde{x}_s}{dt} [u] + \frac{dx_s}{dt} \tilde{x}_s \left[\frac{\partial u}{\partial x} \right] - \tilde{x}_s \left[\frac{df}{du} \frac{\partial u}{\partial x} \right] \right) dt \\
&= - (\tilde{x}_s [G] - v_s [u])|_{t=T} + \int_{\Gamma} -\tilde{x}_s \frac{d}{dt} (v_s [u]) + \frac{dx_s}{dt} \tilde{x}_s v_s \left[\frac{\partial u}{\partial x} \right] - \tilde{x}_s v_s \left[\frac{df}{du} \frac{\partial u}{\partial x} \right] dt
\end{aligned}$$

Since

$$\frac{d}{dt} [u] = \left[\frac{\partial u}{\partial t} \right] + \frac{dx}{ds} \left[\frac{\partial u}{\partial x} \right] = - \left[\frac{df}{du} \frac{\partial u}{\partial x} \right] + \frac{dx}{ds} \left[\frac{\partial u}{\partial x} \right]$$

it follows that these terms cancel if v_s satisfies the equation

$$\frac{dv_s}{dt} = 0,$$

subject to the end condition $v_s = [G] / [u]$ on $t=T$.

Under all of these conditions, the linearised functional reduces finally to

$$\tilde{J} = \iint_{\Omega \setminus \Gamma} v s dx dt.$$

Since $v = v_s$ on either side of the shock, the fact that v_s is constant along the shock means that the adjoint solution has a uniform value along all characteristics leading

backwards from the shock, as well as a constant value along each individual characteristic coming backwards in time from $t=T$.

This result, and the value of the adjoint variables along the shock, can also be re-derived by considering a unit strength point source term in the linearised equation. If a source term $S(x, t)$ is added to the original nonlinear equation, then integrating over Ω yields

$$\int_0^1 u(x, T) - u(x, 0) \, dx + \int_0^T f(u(1, t)) - f(u(0, t)) \, dt = \int_{\Omega} S(x, t) \, dx \, dt.$$

Linearising this, taking account of the linearised shock displacement, gives

$$\int_0^{x_s} \tilde{u}(x, T) \, dx + \int_{x_s}^1 \tilde{u}(x, T) \, dx - (x_s [u])|_{t=T} = \int_{\Omega} s(x, t) \, dx \, dt.$$

Now, for a unit point source on a characteristic which leads to the shock, then the resulting final linear perturbation $\tilde{u}(x, T)$ is zero on both sides of the shock. Hence,

$$\tilde{x}_s(T) = - [u]^{-1}|_{t=T}$$

and the corresponding functional perturbation is

$$\tilde{J} = - (\tilde{x}_s [G])|_{t=T} = \frac{[G]}{[u]} \Big|_{t=T}.$$

Although the adjoint solution $v(x, t)$ is continuous across the shock for $t < T$, with value equal to the shock adjoint variable $v_s(t)$, in general there is not continuity at the final time T . Defining u_- and u_+ to be the values of $u(x, T)$ on either side of the shock, then

$$[G] = \int_{u_-}^{u_+} \frac{dG}{du} \, du,$$

and therefore $v_s(T) = [G]/[u]$ is the average value of $g(x) \equiv dG/du$ over the range of u spanned by the shock. Given the assumed continuity of dG/du , this means that the value of $v_s(T)$ will approach the values of $g(x)$ on either side of the shock in the limit as the shock strength approaches zero.

4 Numerical discretisation

We consider a class of explicit finite volume discretisations of the form

$$\frac{1}{\Delta t} M (U^{n+1} - U^n) + \Delta F^n = 0.$$

Here U^n is the vector of solution values $U_j^n, 0 \leq j \leq J$ at the n^{th} timestep. M is a diagonal mass matrix whose entries are

$$M_{jj} = \begin{cases} \frac{1}{2}(x_1 - x_0) & j = 0, \\ \frac{1}{2}(x_{j+1} - x_{j-1}) & 0 < j < J \\ \frac{1}{2}(x_J - x_{J-1}) & j = J, \end{cases}$$

Given a numerical flux $F_{j+1/2}$ which is a function of both U_j and U_{j+1} , the flux difference ΔF^n is defined as

$$\Delta F_j^n = \begin{cases} F_{1/2}^n - f(u(0, t^n)) & j = 0, \\ F_{j+1/2}^n - F_{j-1/2}^n & 0 < j < J \\ f(u(1, t^n)) - F_{J-1/2}^n & j = J. \end{cases}$$

Note that this uses a weak implementation of the Dirichlet boundary conditions, as opposed to explicitly setting the values of U_0^n and U_J^n . This weak treatment is preferable because it leads to the attractive conservation property

$$M (U^N - U^0) = \Delta t \sum_{n=0}^{N-1} f(u(1, t^n)) - f(u(0, t^n))$$

and a cleaner formulation of the adjoint discretisation.

Having computed the numerical solution, the discrete form of the nonlinear output functional is evaluated as

$$J = \sum_j M_{jj} G(U_j^N).$$

The linearised equations with the inclusion of the source term can be written as

$$\frac{1}{\Delta t} M (\tilde{U}^{n+1} - \tilde{U}^n) + A^n \tilde{U}^n = M S^n. \quad (4.1)$$

In addition, the linearised output functional is

$$\tilde{J} = g^T M \tilde{U}^N \equiv \sum_j \left(\frac{dG}{du} \right)_j^N M_{jj} \tilde{U}_j^N.$$

In formulating the discrete adjoint equations, we follow what is often termed the ‘‘fully discrete’’ approach in which the goal is to define the adjoint equations in such

a way as to obtain exactly the same value for the discrete linearised functional. This is in contrast to the ‘‘continuous adjoint’’ approach which directly discretises the adjoint differential equation, independently of the discretisation of the original nonlinear equation.

Considering to begin with the case in which $S^n = 0$ for $n > 0$, the linear discrete equations, (4.1), may be solved to obtain

$$\tilde{J} = \Delta t g^T M (I - \Delta t M^{-1} A^{N-1}) \dots (I - \Delta t M^{-1} A^2) (I - \Delta t M^{-1} A^1) S^0.$$

This may be re-arranged as

$$\begin{aligned} \tilde{J} &= \Delta t g^T (I - \Delta t A^{N-1} M^{-1}) \dots (I - \Delta t A^2 M^{-1}) (I - \Delta t A^1 M^{-1}) M S^0 \\ &= \Delta t (V^1)^T M S^0, \end{aligned}$$

where V^1 is obtained by solving the discrete adjoint equation

$$\frac{1}{\Delta t} M (V^{n+1} - V^n) + (A^n)^T V^{n+1} = 0, \quad (4.2)$$

subject to the final condition $V^N = g$.

Extending to the general case in which S^n is non-zero at all time levels, the definition of the adjoint variables is unchanged and the resulting expression for the functional is

$$\tilde{J} = \Delta t \sum_{n=0}^{N-1} (V^{n+1})^T M S^n.$$

Note that this is a discrete equivalent of equation (2.3).

Looking in detail at the elements of the matrix A^n , one finds that the discrete adjoint equation for the j^{th} node is

$$\frac{1}{\Delta t} M_{jj} (V_j^{n+1} - V_j^n) + \left(\frac{\partial F_{j+1/2}^n}{\partial U_j^n} \right) (V_{j+1}^{n+1} - V_j^n) + \left(\frac{\partial F_{j-1/2}^n}{\partial U_j^n} \right) (V_j^{n+1} - V_{j-1}^n) = 0.$$

To prove that this is a consistent approximation of the adjoint differential equation, (2.2), we need to note that for consistency the original nonlinear flux function is required to satisfy the condition

$$F_{j+1/2}^n(U_j^n, U_{j+1}^n) = f(u) \quad \text{when} \quad U_j^n = U_{j+1}^n = u.$$

Differentiating this yields

$$\frac{\partial F_{j+1/2}^n}{\partial U_j^n} + \frac{\partial F_{j+1/2}^n}{\partial U_{j+1}^n} = \frac{df}{du} \quad \text{when} \quad U_j^n = U_{j+1}^n = u,$$

and hence

$$\frac{\partial F_{j+1/2}^n}{\partial U_j^n} + \frac{\partial F_{j-1/2}^n}{\partial U_j^n} = \frac{df}{du} \quad \text{when} \quad U_{j-1}^n = U_j^n = U_{j+1}^n = u.$$

It therefore follows that the discrete adjoint equation is a consistent approximation of equation (2.2) when the underlying flow solution is smooth.

We will continue to use the same adjoint discretisation when the flow solution contains a shock. The question to be investigated is whether this will automatically capture the correct adjoint solution in the limit of increasing grid resolution. As a prelude, we note that only $g \equiv dG/du$ enters into the adjoint calculation as initial data, not $[G]$ and so it is not clear that the adjoint calculation has the information necessary to correctly predict the adjoint solution in the neighbourhood of the shock.

5 Numerical tests

The numerical tests are all performed with the Burgers equation for which $f(u) \equiv \frac{1}{2}u^2$. Most of the tests use the initial conditions

$$u(x, 0) = \begin{cases} 1, & x < 0.25 \\ 2 - 4x, & 0.25 \leq x \leq 0.75 \\ -1, & x > 0.75 \end{cases}$$

and boundary conditions $u(0, t) = 1$, $u(1, t) = -1$. As shown in Figure 1, a stationary shock forms at $x=0.5$ at time $t=0.25$. The analytic solution is

$$u(x, t) = \begin{cases} 1, & x < \min(0.25+t, 0.5) \\ \frac{x - 0.5}{t - 0.25}, & \min(0.25+t, 0.5) < x < \max(0.75-t, 0.5) \\ -1, & x > \max(0.75-t, 0.5) \end{cases}$$

To assess the degree to which the solutions are grid converged, numerical results are obtained on two uniform grids with $\Delta x = 0.0025, 0.005$. The corresponding timesteps are $\Delta t = 0.4\Delta x$ giving a maximum CFL number of 0.4.

The output functional uses $G(u) = u^5 - u$. This gives $g(x) = 4$ on either side of the shock. Furthermore, the jump $[G]$ across the shock is equal to zero, so the analytic solution has $v=0$ for all backward travelling characteristics emanating from the shock. Hence the complete adjoint solution is

$$v(x, t) = \begin{cases} 4, & x < t \\ 0, & t < x < 1-t \\ 4, & x > 1-t \end{cases}$$

In the results to be presented, one of the main points of interest will be the computed values for $v(x, t)$ on the characteristics coming from the shock.

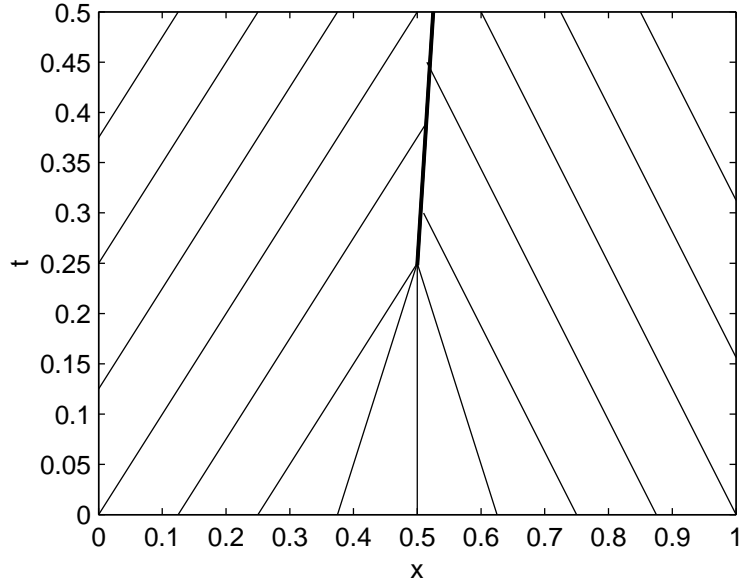


Figure 2: Characteristics with the formation of a slowly moving shock.

To investigate whether a moving shock produces different results, some additional numerical tests use the initial conditions

$$u(x, 0) = \begin{cases} 1, & x < 0.25 \\ 2 - 4x, & 0.25 \leq x \leq 0.7 \\ -0.8, & x > 0.7 \end{cases}$$

with boundary conditions $u(0, t) = 1$, $u(1, t) = -0.8$,

As illustrated in Figure 2, this results in a solution with a slowly moving shock.

$$u(x, t) = \begin{cases} 1, & x < \min(0.25+t, 0.475+0.1t) \\ \frac{x-0.5}{t-0.25}, & \min(0.25+t, 0.475+0.1t) < x < \max(0.7-0.8t, 0.475+0.1t) \\ -0.8, & x > \max(0.7-0.8t, 0.475+0.1t) \end{cases}$$

Using the same functional as before, the corresponding adjoint solution is

$$v(x, t) = \begin{cases} 4, & x < 0.025+t \\ -0.2624, & 0.025+t < x < 0.925-0.8t \\ 1.048 \times 0.8^4, & x > 0.925-0.8t \end{cases}$$

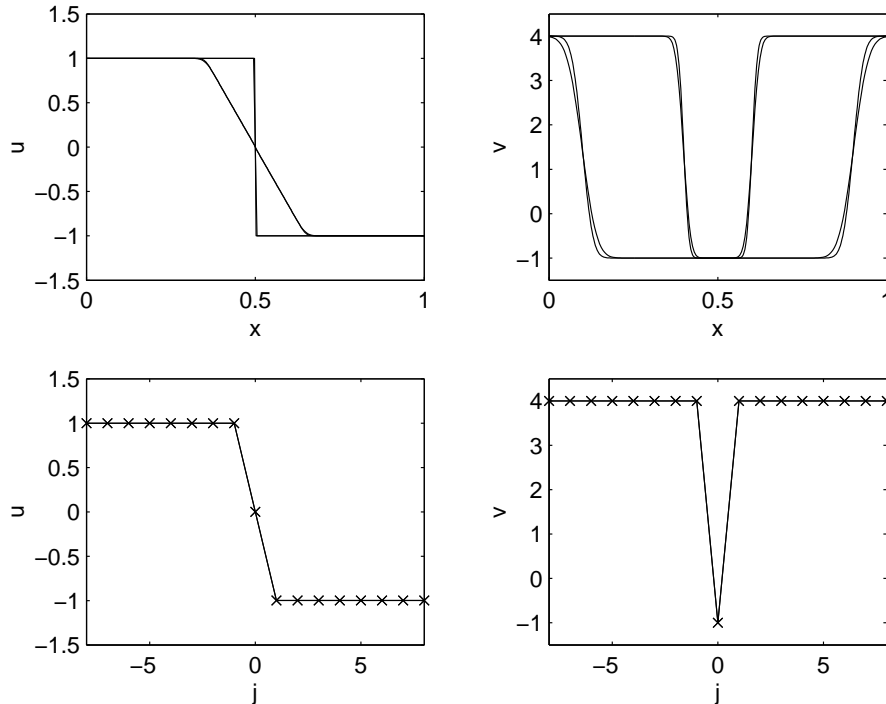


Figure 3: Nonlinear and adjoint solutions obtained with a Riemann flux, for $t=0.1, 0.4$ in the upper plots, and $t=0.5$ in the lower plots.

5.1 Riemann flux

The first results use a first order Riemann numerical flux function [LeV92],

$$F(u_1, u_2) = \frac{1}{2} \max \left((\max(0, u_1))^2, (\min(0, u_2))^2 \right).$$

The upper two plots in Figure 3 show the nonlinear and adjoint solution at times $t = 0.1, 0.4$. There is very little difference between the solutions for the two grids. However it is very clear that the adjoint solution is completely wrong in the region emanating from the shock, where the computed value is approximately equal to -1 .

The cause for this incorrect value can be seen in the lower two plots which show the nonlinear and adjoint solutions at the final time $t = 0.5$, plotted versus node number relative to the central node at $x = 0.5$. It is seen that on both grids the nonlinear solution has a single shock point at which $u = 0$. For this point the corresponding adjoint value is $g = dG/du(0) = -1$, and a detailed examination of the matrix A reveals that this value is propagated backward in time along the length of the shock, and along any characteristic which propagates out of the shock.

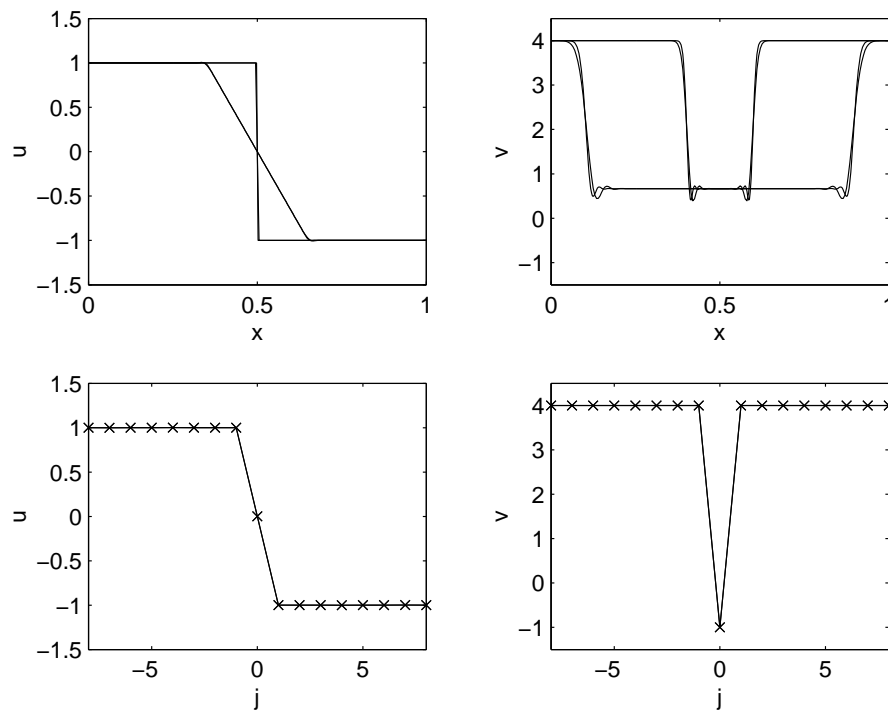


Figure 4: Nonlinear and adjoint solutions obtained with a Lax-Friedrichs flux with smoothing $\mu=0.25$, for $t=0.1, 0.4$ in the upper plots, and $t=0.5$ in the lower plots.

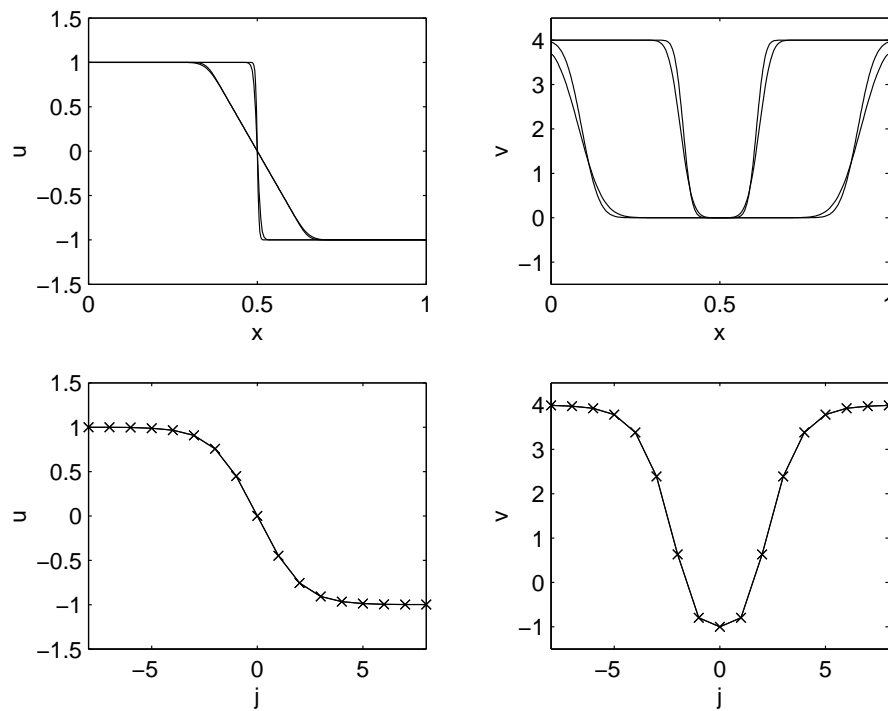


Figure 5: Nonlinear and adjoint solutions obtained with a Lax-Friedrichs flux with smoothing $\mu=1.0$, for $t=0.1, 0.4$ in the upper plots, and $t=0.5$ in the lower plots.

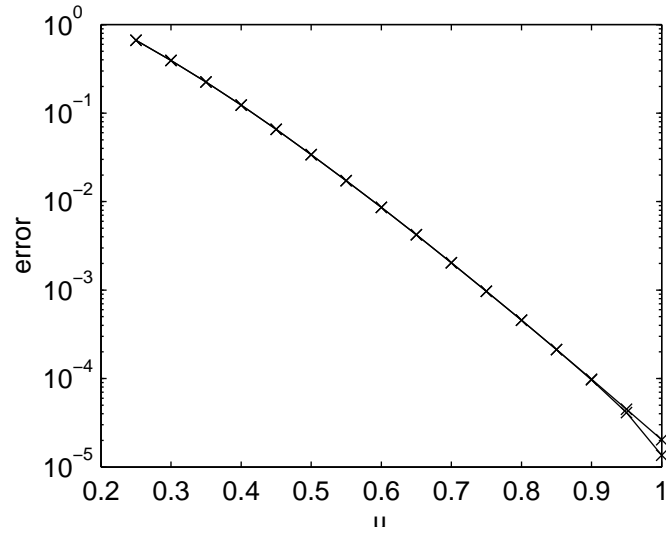


Figure 6: Error in the computed value for $v(0.5, 0)$ as a function of the numerical smoothing coefficient μ .

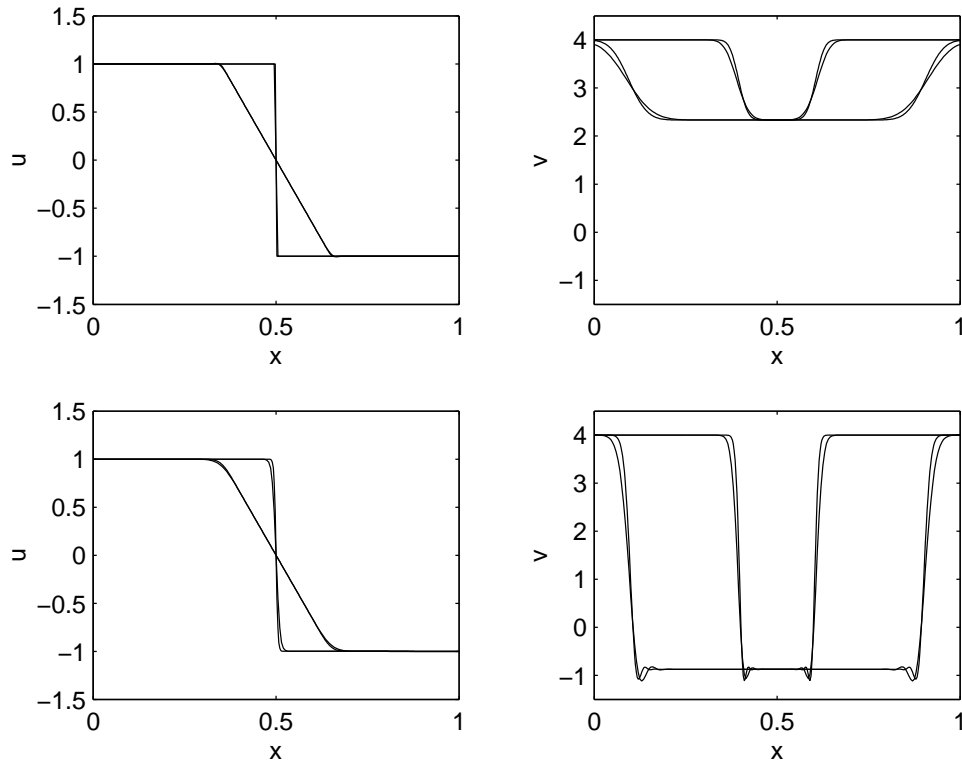


Figure 7: Solutions at $t = 0.1, 0.4$ using the Lax-Friedrichs flux with different levels of smoothing in the nonlinear and adjoint calculations. Upper results: $\mu(\text{nonlinear}) = 0.25$, $\mu(\text{adjoint}) = 1.0$. Lower results: $\mu(\text{nonlinear}) = 1.0$, $\mu(\text{adjoint}) = 0.25$.

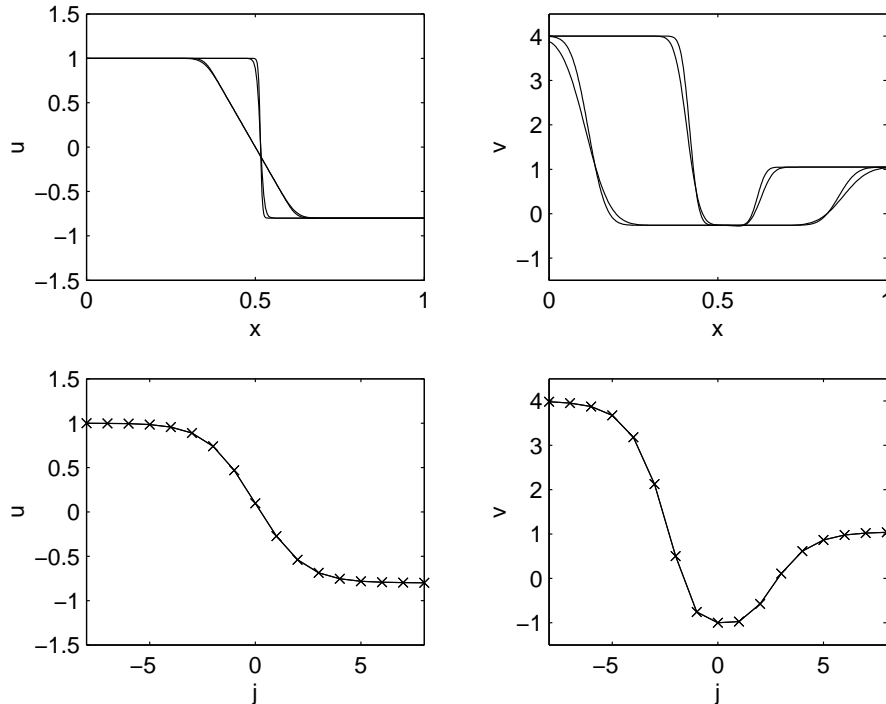


Figure 8: Nonlinear and adjoint solutions for the moving shock test case, using the Lax-Friedrichs flux with smoothing $\mu = 1.0$, for $t=0.1, 0.4$ in the upper plots, and $t=0.5$ in the lower plots.

Figure 6 plots the error in the computed value for $v(0.5, 0)$ versus the value of the smoothing coefficient μ . It appears from these results that the error decreases exponentially with the value of μ and hence the number of grid points across the shock.

Figure 7 presents results obtained by using different values for μ in the nonlinear and adjoint calculations. The upper results use $\mu = 0.25$ for the nonlinear calculations, and $\mu = 1.0$ for the adjoint calculation. The higher value for μ in the adjoint calculation leads to rapid diffusion bringing into the shock region the larger values for the adjoint solution $v(x, t)$ on either side of the shock, leading to incorrect values in the shock region. The lower results use $\mu = 1.0$ for the nonlinear calculations, and $\mu = 0.25$ for the adjoint calculation. The lower value for μ in the adjoint calculation leads to very little diffusion, and so the adjoint solution value $g = -1$ at the centre of the smeared shock is convected backwards in time leading to $v(x, t) \approx -1$ throughout the shock region. These results show the importance of using the same value of μ in both calculations, so that the adjoint discretisation corresponds correctly to the linearisation of the nonlinear discretisation.

The final results in Figures 8 and 9 are for the moving shock test case. The index j in the lower plots in Figure 8 is relative to the node at the centre of the shock at the final time. Figure 9 shows that there is again exponential convergence in the adjoint solution $v(0, 5, 0)$ as the smoothing is increased. Thus, this phenomenon does not depend on the shock being stationary.

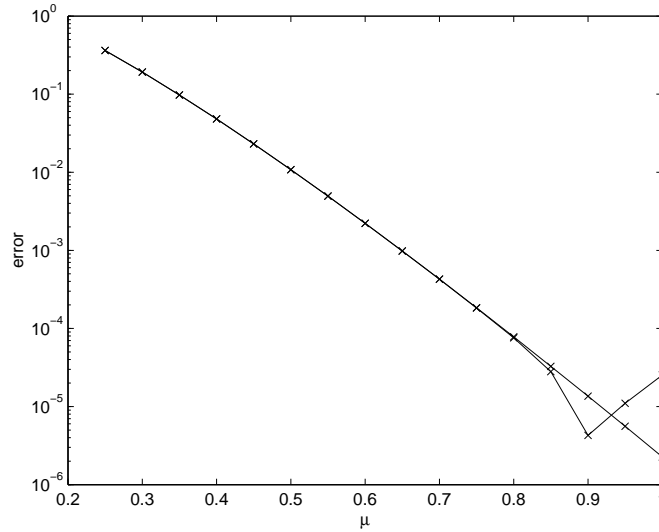


Figure 9: Error in the computed value for $v(0.5, 0)$ for the moving shock testcase, as a function of the numerical smoothing coefficient μ .

6 Discussion

One clear conclusion from these numerical results is that there must be consistency between the nonlinear and adjoint calculations regarding the level of numerical smoothing. Also, for convergence it is necessary that as the grid resolution improves, the numerical smoothing varies in a way which increases the number of points across the shock, while at the same time the overall width of the shock decreases.

To understand why this latter point is fundamental, and not just a feature of the particular numerical experiments conducted, we need to consider the information supplied to the adjoint code. The analytic solution has a value along the shock which depends on the jump $[G(u)]$ across the shock at the final time $t = T$. However, the end conditions for the numerical adjoint solution are given by the values of dG/du for the final values of u obtained from the nonlinear calculation. These means that the numerical solution must implicitly evaluate $[G(u)]$ by some process which effectively integrates dG/du across the smeared shock. For this to be done accurately requires adequate resolution of the variation in dG/du .

This point is illustrated in Figure 10. The smoother of the two curves is $G(u) = u^5 - u$, the objective function in the numerical experiments. The symbols correspond to the values of u at the final time $t = T$ in Figure 5. The second curve is $G(u) = u^5 - u + \tanh 20(u - 0.2)$. This function has almost identical gradient values at the indicated sampling points, and therefore produces a numerical adjoint solution which is visually indistinguishable from Figure 5. However, the analytic solution has a different jump in $G(u)$ across the shock, and so the analytic solution is quite different. This shows that for any numerical discretisation with a fixed number of points across the shock, it is easy to construct an objective function for which the numerical adjoint solution will not converge.

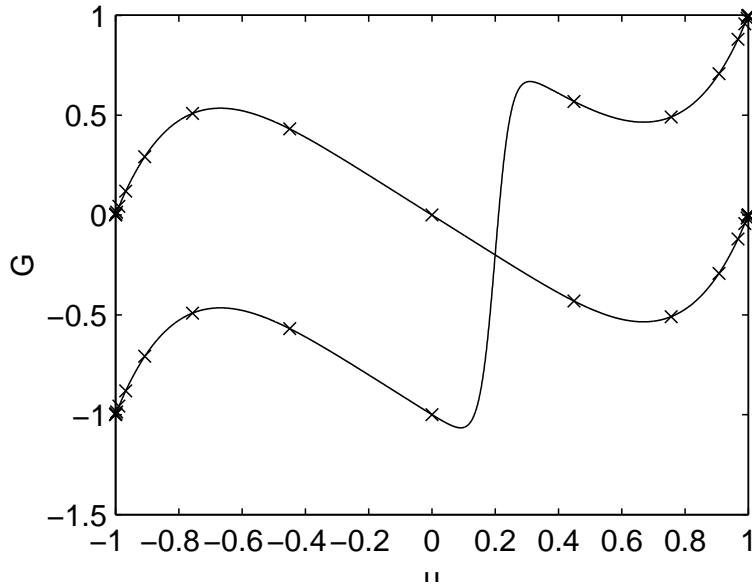


Figure 10: Two objective functions $G(u)$.

Effectively, what the numerical computation is implicitly doing is to obtain the jump $[G(u)]$ through the integral of its gradient.

$$[G(u)] = \int_{u^-}^{u^+} \frac{dG}{du} du = \int_{-\infty}^{\infty} \frac{dG}{du} \frac{\partial u}{\partial x} dx.$$

It is therefore interesting to note that the trapezoidal integration of an analytic function $w(x)$ which decays exponentially as $|x| \rightarrow \infty$ has an error which decreases exponentially with the reciprocal of the uniform mesh spacing [Ste81]. This may be related to the exponential dependence of the adjoint error on the level of numerical smoothing, and hence the number of points in the smeared shock.

A final observation concerns the magnitude of the errors likely to be encountered in practical aerodynamic computations. At the end of section 3 it was noted that $[G(u)]/[u]$ represents the average value of dG/du across the shock, so in the case of weak shocks this will be very close to the values of $g(x)$ on either side of the shock. What can be considered a ‘weak’ shock will depend on the variation in dG/du across the shock. However, for the purposes of aeronautical design optimisation, which is one of the primary motivations for this study, it seems likely that if the normal Mach number entering the shock is less than 1.1, or even perhaps as much as 1.2, then the errors will not be significant. This belief is based in part on the fact that adjoint methods have been used very successfully for transonic design applications without observing any difficulties associated with the shock.

References

- [AV99] W.K. Anderson and V. Venkatakrishnan. Aerodynamic design optimization on unstructured grids with a continuous adjoint formulation. *Computers & Fluids*, 28(4-5):443–480, 1999.
- [BJ98] F. Bouchut and F. James. One-dimensional transport equations with discontinuous coefficients. *Nonlinear Analysis*, 32:891–933, 1998.
- [BR01] R. Becker and R. Rannacher. An optimal control approach to error control and mesh adaptation. In A. Iserles, editor, *Acta Numerica 2001*. Cambridge University Press, 2001.
- [Gil96] M.B. Giles. Analysis of the accuracy of shock-capturing in the steady quasi-1D Euler equations. *International Journal of Computational Fluid Dynamics*, 5(2):247–258, 1996.
- [Gil02] M.B. Giles. Discrete adjoint approximations with shocks. In T. Hou and E. Tadmor, editors, *Proceedings of HYP2002*. Springer-Verlag, 2002.
- [GP98] M.B. Giles and N.A. Pierce. On the properties of solutions of the adjoint Euler equations. In M. Baines, editor, *Numerical Methods for Fluid Dynamics VI*. ICFD, Jun 1998.
- [GP00] M.B. Giles and N.A. Pierce. An introduction to the adjoint approach to design. *Flow, Turbulence and Control*, 65(3/4):393–415, 2000.
- [GP01] M.B. Giles and N.A. Pierce. Analytic adjoint solutions for the quasi-one-dimensional Euler equations. *Journal of Fluid Mechanics*, 426:327–345, 2001.
- [HCL94] K.C. Hall, W.S. Clark, and C.B. Lorence. A linearized Euler analysis of unsteady transonic flows in turbomachinery. *Journal of Turbomachinery*, 116:477–488, 1994.
- [Jam95] A. Jameson. Optimum aerodynamic design using control theory. In M. Hafez and K. Oshima, editors, *Computational Fluid Dynamics Review 1995*, pages 495–528. John Wiley & Sons, 1995.
- [JRB95] C. Johnson, R. Rannacher, and M. Boman. Numerics and hydrodynamic stability – toward error control in computational fluid dynamics. *SIAM Journal of Numerical Analysis*, 32(4):1058–1079, 1995.
- [LeV92] R.J. LeVeque. *Numerical methods for conservation laws*. Lectures in Mathematics ETH Zürich. Birkhäuser Verlag, 2nd edition, 1992.
- [LG94] D.R. Lindquist and M.B. Giles. Validity of linearized unsteady Euler equations with shock capturing. *AIAA Journal*, 32(1):46, 1994.

- [MS98] P. Monk and E. Süli. The adaptive computation of far field patterns by a posteriori error estimates of linear functionals. *SIAM Journal of Numerical Analysis*, 36(1):251–274, 1998.
- [PG00] N.A. Pierce and M.B. Giles. Adjoint recovery of superconvergent functionals from PDE approximations. *SIAM Review*, 42(2):247–264, 2000.
- [Ste81] F. Stenger. Numerical methods based on Whittaker cardinal, or sinc functions. *SIAM Review*, 23:165–224, 1981.
- [SW98] K. Sreenivas and D.L. Whitfield. Time- and frequency-domain numerical simulation of linearized Euler equations. *AIAA Journal*, 36(6):968–975, 1998.
- [Tad91] E. Tadmor. Local error estimates for discontinuous solutions of nonlinear hyperbolic equations. *SIAM Journal of Numerical Analysis*, 28:891–906, 1991.
- [Ulbr02a] S. Ulbrich. Adjoint-based derivative computations for the optimal control of discontinuous solutions of hyperbolic conservation laws. *Systems & Control Letters*, to appear, 2002.
- [Ulbr02b] S. Ulbrich. A sensitivity and adjoint calculus for discontinuous solutions of hyperbolic conservation laws with source terms. *SIAM Journal of Control and Optimization*, to appear, 2002.